GEOPHYSICS, VOL. 74, NO. 6 (NOVEMBER-DECEMBER 2009); P. A75–A80, 5 FIGS.
10.1190/1.3213533

Nonstationary phase estimation using regularized local kurtosis maximization

Mirko van der Baan[1] and Sergey Fomel[2]

ABSTRACT

Phase mismatches sometimes occur between final processed seismic sections and zero-phase synthetics based on well logs — despite best efforts for controlled-phase acquisition and processing. Statistical estimation of the phase of a seismic wavelet is feasible using kurtosis maximization by constant-phase rotation, even if the phase is nonstationary. We cast the phase-estimation problem into an optimization framework to improve the stability of an earlier method based on a piecewise-stationarity assumption. After estimation, we achieve space-and-time-varying zero-phasing by phase rotation.

INTRODUCTION

Controlled-phase acquisition and processing play an important role in current acquisition and processing strategies (Trantham, 1994). Despite best efforts to control the phase of the wavelet during the entire acquisition and processing sequence, phase mismatches regularly occur between final processed data based on deterministic zero-phase shaping and zero-phase synthetics created from well logs. Existing well logs act here as ground truth, and a further phase correction is applied to the data such that they match the zero-phase synthetics.

Unfortunately, well logs are not always available, and different wells can predict different phase corrections or the phase mismatch can vary with time. Statistical wavelet-estimation methods do not require well logs and analyze the seismic data directly. Van der Baan (2008) recently developed such a statistical method suitable for estimating nonstationary nonminimum-phase wavelets by extending earlier work by Levy and Oldenburg (1987), Longbottom et al. (1988), and White (1988).

These authors search for a constant-phase rotation that renders the data maximally non-Gaussian. Their statistical methods estimate phase using a consequence of the central limit theorem: Convolution of any filter with a time series, which is white with respect to all statistical orders, renders the amplitude distribution of the outcome more Gaussian (Donoho, 1981).

If we assume that the seismic wavelet can be described adequately by a frequency-dependent amplitude spectrum but a constant phase, then the phase can be found by phase rotating the seismic data until they become maximally non-Gaussian. The constant-phase assumption seems to hold in practice except for dispersive wavelets (van der Baan and Pham, 2008).

Van der Baan (2008) extends the constant-phase rotation method to handle nonstationary (e.g., time-varying) data and shows how to extract the time-varying wavelet, which can serve as a more familiar quality-control tool for interpreters than phase information alone. His approach involves moving analysis windows. In each window, a single constant-phase wavelet is estimated by kurtosis maximization. Linear interpolation between evaluation positions then yields the desired wavelet phase and amplitude spectrum at each time instant. This approach thus invokes a piecewise-stationarity assumption; the wavelet and its phase are assumed to be constant within individual analysis windows. Furthermore, rapid variations in phase estimates are not uncommon in the previous method if the chosen window length is too short. This renders the moving-window technique less suitable as an interpretational tool, for instance, to highlight subtle stratigraphic features.

In this paper, we show how to eliminate the piecewise-stationarity assumption by casting the problem into the framework of local attributes (Fomel, 2007a), where the problem of local kurtosis maximization within individual windows is recast as regularized least-squares optimization across the entire seismic section (Fomel et al., 2007). Tests with synthetic and field data sets demonstrate that the proposed extension also makes the previous method more robust with respect to smaller window sizes or regularization lengths.

Manuscript received by the Editor 17 April 2009; revised manuscript received 25 May 2009; published online 4 December 2009.
[1]University of Alberta, Department of Physics, CEB, Edmonton, Alberta, Canada. E-mail: mirko.vanderbaan@ualberta.ca.
[2]University of Texas at Austin, John A. and Katherine G. Jackson School of Geosciences, Bureau of Economic Geology, University Station, Austin, Texas, USA. E-mail: sergey.fomel@beg.utexas.edu.

We demonstrate how a statistical analysis provides pertinent information about the data that can be used for zero-phasing, as a quality control tool to check deterministic phase corrections, or even as an interpretational tool for highlighting areas of potential interest. First we describe the method in detail. Then we show both a realistic synthetic and two real data examples, and finally, we briefly discuss the underlying statistical assumptions and a performance comparison between statistical wavelet estimates and deterministic ones originating from seismic-to-well ties.

METHOD

We apply a series of constant-phase rotations to the data to estimate the desired wavelet phase. The angle where the resulting output is maximally non-Gaussian corresponds to the desired zero-phase trace (Levy and Oldenburg, 1987; Longbottom et al., 1988; White, 1988; van der Baan, 2008). The rotated trace $x_{\text{rot}}(t)$ can be computed from the original trace $x(t)$ by

$$x_{\text{rot}}(t) = x(t)\cos\,\phi + H[x(t)]\sin\,\phi, \tag{1}$$

where ϕ is the phase rotation angle and $H[\,.\,]$ denotes the Hilbert transform. Note that equation 1 allows for both a constant and time-dependent rotation angle ϕ.

We measure the maximum deviation from a Gaussian time series using the kurtosis, a fourth-order statistical measure already used by Wiggins (1978) in his blind deconvolution algorithm. Kurtosis κ is computed for a discrete time series $x(t)$ using

$$\kappa[x] = \frac{E[x^4]}{(E[x^2])^2} - 3, \tag{2}$$

where $E[\,.\,]$ indicates the expectation (i.e., averaging) operator applied on data x. Thus, maximizing the kurtosis reveals the desired wavelet phase. It is equal to $-\phi_{\text{kurt}}$, the rotation angle at the maximum kurtosis value. This angle is easiest estimated using a grid search with test angles ϕ between $-90°$ and $90°$.

Van der Baan (2008) divides a seismic section into partially overlapping time windows and estimates the optimum phase-rotation angle ϕ in each individual window. Linear interpolation of phase estimates then obtains the phase at each time sample thus softening the invoked piecewise-stationarity assumption. Large overlaps in the analysis windows are required to render the method stable and for quality control on the optimum window size.

The recorded signal $x(t)$ can be considered as a single realization of a stochastic process. This means that we cannot compute the local kurtosis $\kappa[x](t)$ at each individual time sample t without invoking ergodicity; ensemble averaging then can be replaced by spatial or temporal averaging (van der Baan, 2001). One possibility then consists of assuming piecewise stationarity, that is, by computing the kurtosis within some time window leading again to the method of van der Baan (2008). Alternatively, we can obtain a local estimate by formulating this as a regularized optimization problem (Fomel, 2007b).

Fomel et al. (2007) factorize the kurtosis $\kappa[x]$, equation 2, as follows:

$$\kappa[x] = \left(\frac{1}{E[x^2]}\right)\left(\frac{E[x^4]}{E[x^2]}\right) - 3 = p^{-1}q^{-1} - 3. \tag{3}$$

Furthermore, the constant p is the global solution of the least-squares minimization problem

$$L[p] = \min_p \sum_t \{x^2(t) - p\}^2, \tag{4}$$

and constant q is the global solution of the least-squares minimization problem

$$L[q] = \min_q \sum_t \{1 - qx^2(t)\}^2. \tag{5}$$

Local estimation of the time-varying quantities $p(t)$ and $q(t)$ is then possible by solving independently the following two optimization problems (Fomel et al., 2007):

$$L[p](t) = \min_{p(t)}\left(\sum_t \{x^2(t) - p(t)\}^2 + R[p(t)]\right) \tag{6}$$

and

$$L[q](t) = \min_{q(t)}\left(\sum_t \{1 - q(t)x^2(t)\}^2 + R[q(t)]\right). \tag{7}$$

Finally, the local kurtosis $\kappa[x](t)$ is given by $\kappa[x](t) = 1/\{p(t)q(t)\} - 3$, as suggested by equation 3.

To avoid trivial solutions and to stabilize the inverse problem, we impose a regularization constraint $R[\,.\,]$. Several constraints are feasible, including smoothness options [e.g., minimizing first derivatives of $p(t)$ and $q(t)$]. In our case, we apply shaping regularization and invoke triangular smoothing of the estimates $p(t)$ and $q(t)$ within each internal iteration in a conjugate-gradient approach (Fomel, 2007b). A triangle shaper uses local predictions from both left and right neighbors of a sample and averages them using triangle weights. Different triangle sizes can be used for regularization in the time and spatial dimensions.

After inverting for the time-varying phase $\phi_{\text{kurt}}(t)$ obtained by kurtosis maximization, we can apply phase-only deconvolution using equation 1. We also note that wavelet estimation becomes straightforward once the phase is known because only the amplitude spectrum is left to be estimated. This can be done by (1) averaging the amplitude spectra of all traces in each time window and (2) multiplying the averaged window in the time domain by a Hanning taper for enhanced robustness, while (3) ensuring that the amplitude at the Nyquist frequency remains zero. In the frequency domain, the final estimated wavelet then is given by

$$W_t(f) = |W_{\text{av},t}(f)|\exp\{-i\phi_{\text{kurt}}(t)\text{sgn}(f)\}, \tag{8}$$

where $|W_{\text{av},t}|$ is the averaged amplitude spectrum, $\phi_{\text{kurt}}(t)$ is the constant-phase angle determined by evaluating the kurtosis at discrete time t, and sgn(.) is the sign function. These wavelets then can be used for time-varying amplitude-and-phase deconvolution using the procedure outlined in van der Baan (2008).

EXAMPLES

In this section, we provide examples of applying the proposed technique and compare them with results of the previous moving-window approach.

Synthetic example

To illustrate the whole procedure, we use a realistic synthetic example composed of a super-Gaussian reflectivity convolved with two superposed Ricker wavelets with time-varying peak frequencies

and phases. The amplitude distribution of a super-Gaussian signal has longer tails and a sharper peak than that of a Gaussian signal with equal variance. At zero time, the composite wavelet has peak frequencies at 30 and 60 Hz and a constant phase of −45°, which linearly changes to peak frequencies at 15 and 30 Hz and a constant phase of + 45° at the bottom of the recording. The peak frequencies thus are halved from top to bottom, and a total phase rotation of 90° occurs. Figure 1a displays the true wavelet at various times, and Figure 2a and b shows the reflectivity series and resulting seismic input data. This example is challenging because both the amplitude spectrum and phase of the composite wavelet are highly nonstationary.

Figure 1b and c shows the extracted wavelets, and Figure 1d displays the estimated wavelet phase. The phase is estimated using both the previously developed moving-window approach employing a 67% overlap between windows and the described regularized inversion technique. The extracted and instantaneous wavelets compare well for both methods, as do the estimated and averaged phases, yet the regularized approach leads to less fluctuations in the phase estimates with a more natural appearance. It should be noted that phase perturbations of up to 20° are difficult to detect by eye.

Reducing the number of windows from 12 to nine in the moving-window approach leads to less fluctuations in the resulting phase estimates, yet the regularized estimates remain smoother and with smaller deviations from the true trend. The moving-window approach is therefore more sensitive to the chosen window length despite the 67% overlap between adjacent windows.

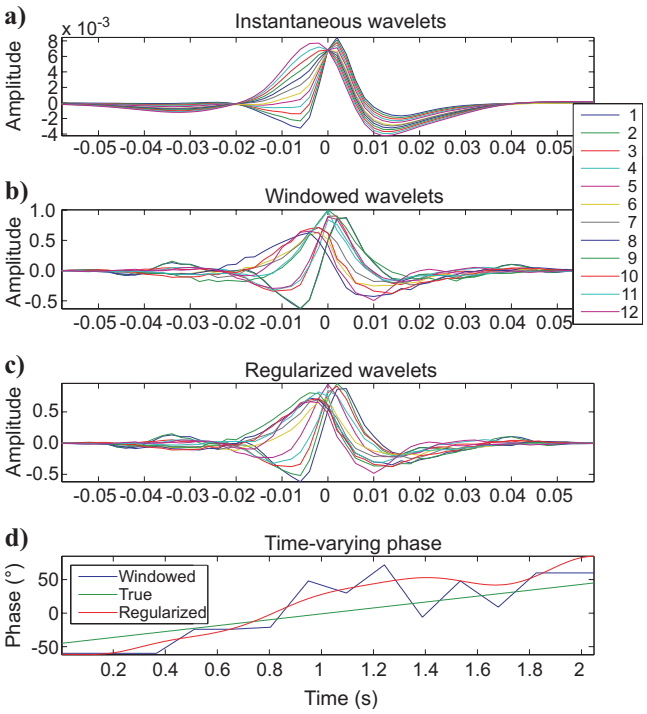

Figure 1. Wavelet-estimation results for the synthetic example. (a) The true wavelet is strongly nonstationary. Instantaneous wavelets are shown at 12 timings, numbered 1–12 with increasing time. Extracted wavelets using (b) moving overlapping windows and (c) local regularized kurtosis estimation. (d) Estimated phases using both methods compared with the true phase. The regularized local kurtosis maximization is more stable than a windowed approach.

A constant-phase rotation on a monofrequency signal amounts to a simple time shift of the entire trace. Applying a time-varying phase rotation on a seismic signal often results in a gentle squeezing, or stretching, of the time series. Phase mismatches on continuous sequences of events thus might give the impression that a timing error is occurring. Only if an isolated event is detected can it become possible to see whether the phase rotation is done properly because a zero-phase wavelet is symmetric. This is evident in Figure 2c-e, which displays the resulting traces after phase-only deconvolution. A comparison with the true zero-phase trace demonstrates again that the regularized phase estimate is more accurate (e.g., at 1.4 s).

Data application 1

Next we consider the same stacked section as in van der Baan (2008), which has known phase problems. Phase has been estimated using the method outlined above. Triangular shaping employs 100 time samples (400 ms) and 50 traces. Figure 3 displays the data before and after phase corrections. The waveforms in the corrected data are more symmetric, which is a characteristic feature of zero-phase data. This can be seen best in the zoomed-in areas in Figure 3c and d.

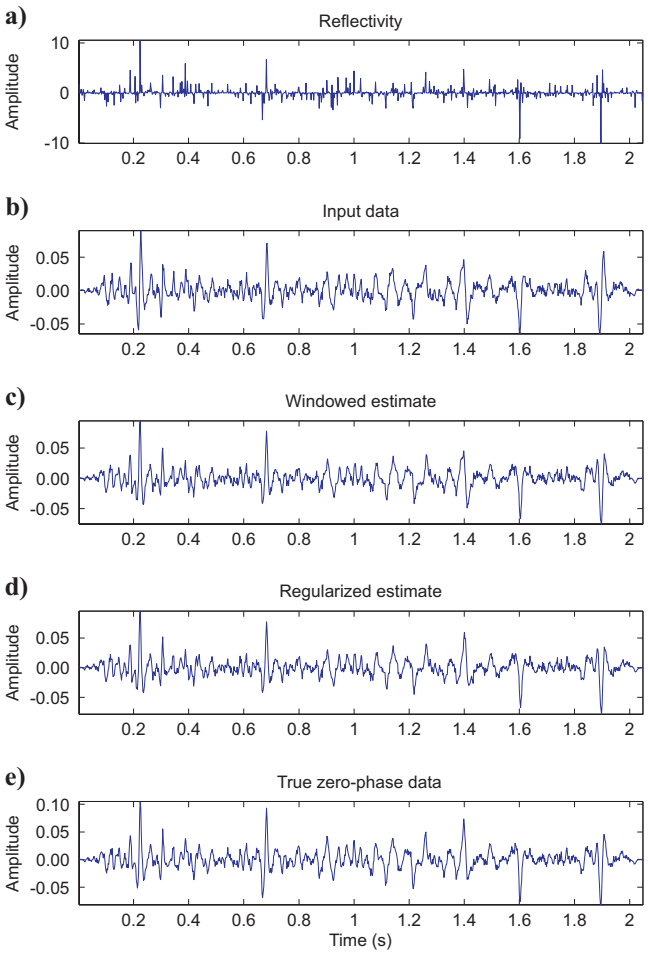

Figure 2. Phase-only deconvolution results for the synthetic example. (a) Reflectivity series, (b) input data with added noise, results after (c) windowed phase estimation, (d) regularized phase estimation, and (e) true zero-phase data. The regularized estimates perform better, in particular at about 1.4 s.

Figure 4 shows the associated phase angles and, for quality-control purposes, the maximum and minimum kurtosis values found and their ratio. Strong temporal and lateral phase variations are visible. The lateral averages agree broadly with the results displayed in Figure 5c of van der Baan (2008) showing a steplike change in the wavelet phase from $-78°$ in the top 1 s, $-40°$ between 1.5 and 3 s, and $-20°$ at 4 s. Relative kurtosis variations range between 1 and 1.22, which is low. However, both the highest relative and absolute kurtosis values are found near the ocean bottom and the prominent dipping layer at 2.5 s, which boosts our confidence that the phase angles are estimated correctly. In addition, the resulting seismic section after phase correction looks reasonable with many symmetric waveforms (Figure 3).

Data application 2

Finally, we consider a stacked section from the Boonsville data set (Hardage et al., 1996), where zero-phasing already has been applied. We include this second data set to illustrate that phase estimation may also have potential applications in seismic interpretation and data analysis.

Figure 5 displays the stacked section and the estimated phase angles. Triangular shaping involved 50 time samples (100 ms) and 15 traces. These small values are set intentionally to emphasize areas where rapid phase variations occur, which we believe reflect changes in the local geology instead of acquisition or processing artifacts, as shown in the previous example. We are confident in our belief be-

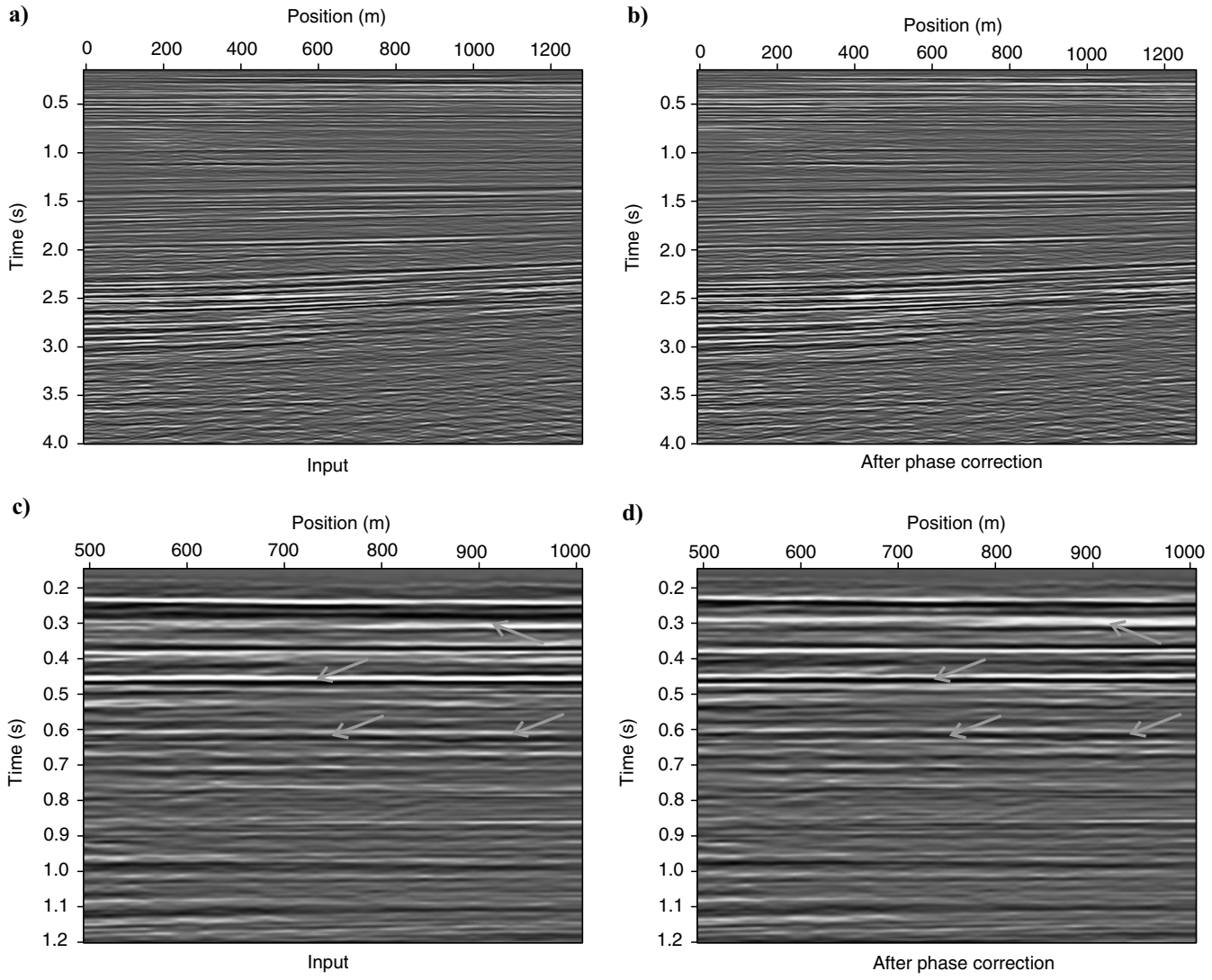

Figure 3. Phase-only deconvolution results for the first real data example. (a) Original data; (b) outcome after space-and-time-varying rotation. Closeup on (c) the original and (d) the phase-corrected result, respectively. Several phase rotations are visible, indicated by gray arrows. Data are courtesy of Shell.

cause imposing large lateral regularization in the inversion leads to phase estimates, which are nearly constant in time with an average of −4°.

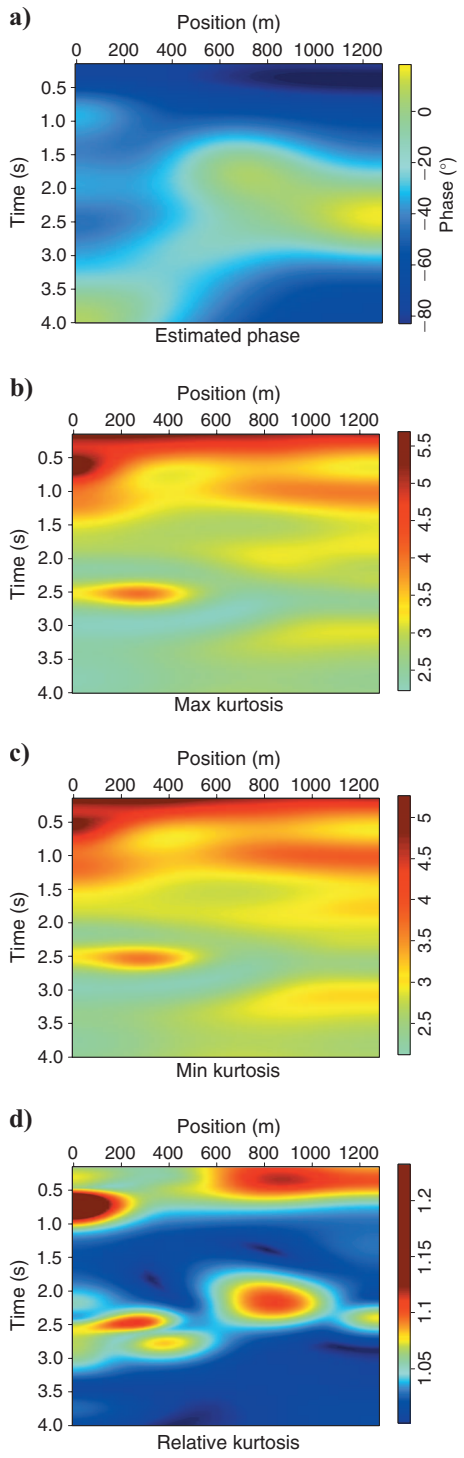

Figure 4. Phase estimates and kurtosis values for the first real data example. (a) Estimated phase at each data point; (b) maximum kurtosis values; (c) minimum kurtosis values; (d) ratio of maximum and minimum kurtosis.

Nearly all phase estimates are less than 20°, and the stacked section after phase-only deconvolution is highly similar to the original. The most dramatic phase rotations occur at the upper left and right corners at 0.3 s and within the plumelike structure originating from the bottom between traces 50 and 90. This area includes the small synclinal dip on the major reflector starting at 1.1 s on the left. Such lateral variations in estimated phase angles can, for instance, be induced by subtle changes in thin-bed layering and their reflectivity response. Nonstationary phase analysis thus can serve as a useful tool to highlight variations in local geology.

DISCUSSION

The described wavelet and phase-estimation technique assumes that the earth's reflectivity series has a white non-Gaussian distribution. The non-Gaussian character of the reflection coefficients is demonstrated by well-log analyses (Walden and Hosken, 1986). On the other hand, it is unlikely that the earth's reflectivity series is white at all depths because this implies that there is no correlation between geologic processes occurring over time (i.e., current geologic processes would not be influenced by the recent past). Indeed, it is known that the earth's reflectivity series is blue instead of white, thus lacking low frequencies (Walden and Hosken, 1985), yet this nonwhiteness generally is considered a second-order problem, which is remedied easily if local well logs exist (Saggaf and Robinson, 2000; Browaeys and Fomel, 2009). Saggaf and Robinson (2000) describe several workflows on how well logs can be used to correct for stationary nonwhite reflectivity series. We recommend applying any nonwhiteness corrections prior to nonstationary phase estimation to better honor the invoked whiteness assumption. Van der Baan (2008) provides more background on the assumptions that underlie the described wavelet-estimation technique.

An isolated thin bed such as a high-velocity chalk marker leads to a seismic response with an approximately 90° phase shift. Zeng and Backus (2005) argue in favor of 90° (rather than zero-phase) wavelets for interpreting the seismic response of thin layers. To achieve the result that they advocate, it is sufficient to apply a 90° phase shift to the output of our method. An irregular sequence of thin beds of varying thicknesses, on the other hand, is unlikely to display the same characteristic response. It is in such an environment that seismic phase analysis is most likely to help detect subtle stratigraphic features including pinch-outs and variations in turbidite and coal sequences, meandering channels, and carbonate reefs.

A justification to employ statistical methods to estimate the wavelet phase and amplitude spectrum is presented by Edgar and van der Baan (2009). These authors compare statistical wavelet estimates obtained directly from the data with deterministic wavelets resulting from seismic-to-well ties for three marine data sets. In all cases, they found that the phase of the resulting wavelets is in close agreement, yet the deterministic seismic-to-well tie wavelets depict more sidelobes and had a more complex character. They conclude that the simpler character of the statistical wavelet estimates looked more realistic and that the extra sidelobes in the deterministic estimates could be introduced to improve the seismic-to-well ties. Thus, these are attributed to a nonphysical transfer function.

We recommend that kurtosis maximization by constant-phase rotation is incorporated as a routine step in seismic data-processing flows. It can reveal the presence of nonstationary nonminimum-phase wavelets without the need for well control. A statistical analysis provides pertinent information about the data that can be used for

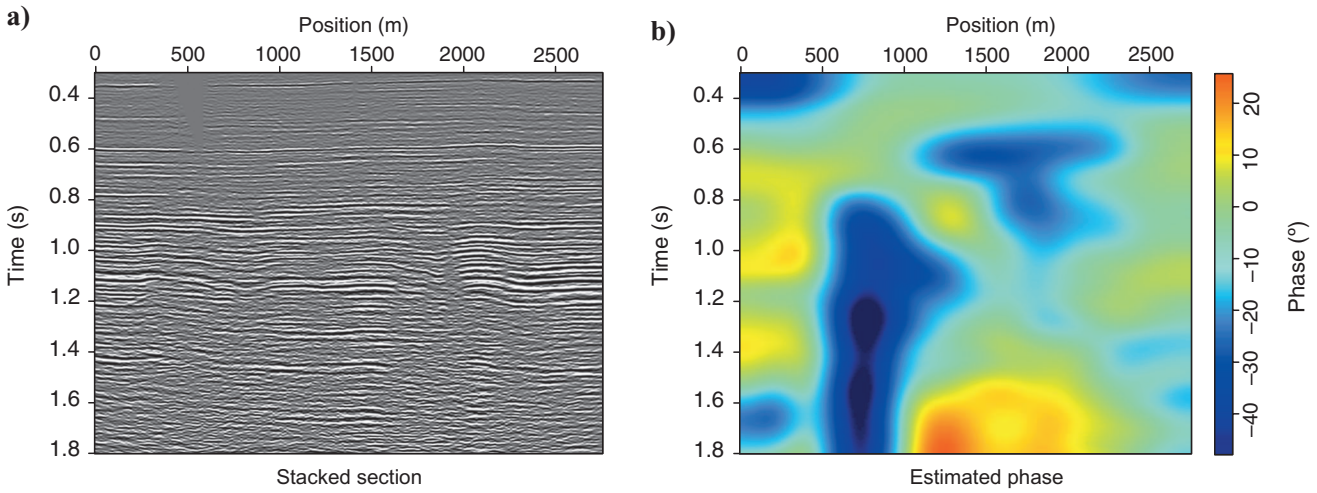

Figure 5. Phase estimation as an interpretational tool. (a) Stacked section (the Boonsville data set). (b) Estimated phase at each data point. Lateral variations in the estimated phase angles indicate areas along major reflectors, where a change in the reflectivity response occurs, e.g., because of the presence of subtle stratigraphic features.

zero-phasing, as a quality control tool to check deterministic phase corrections, or even as an interpretational tool for highlighting areas of potential interest.

CONCLUSIONS

Kurtosis maximization by constant-phase rotation is a useful tool for nonstationary phase estimation. Casting this method into an optimization framework leads to more robust phase estimates than a simpler approach employing individual overlapping analysis windows. The incorporation of shaping regularization in the inversion allows for the use of shorter analysis windows and provides more confidence in obtained phase estimates. The developed technique thus can be used not only to extract nonstationary seismic wavelets suitable for deconvolution but also as an interpretional tool to highlight areas of subtle stratigraphic variations in the local geology.

ACKNOWLEDGMENTS

The first author acknowledges Shell EP Europe for permission to use the data set for the first field data example. We are also grateful to Deyan Draganov, Arnaud Huck, and two anonymous reviewers for their feedback and constructive comments.

REFERENCES

Browaeys, T. J., and S. Fomel 2009, Fractal heterogeneities in sonic logs and low-frequency scattering attenuation: Geophysics, **74**, no. 2, WA77–WA92.

Donoho, D., 1981, On minimum entropy deconvolution, *in* D. F. Findley, ed., Applied time series analysis II, 565–608, Academic Press.

Edgar, J. A., and M. van der Baan, 2009, How reliable is statistical wavelet estimation?: 71st Conference and Exhibition, EAGE, Extended Abstracts, V003.

Fomel, S., 2007a, Local seismic attributes: Geophysics, **72**, no. 3, A29–A33.

——— 2007b, Shaping regularization in geophysical-estimation problems: Geophysics, **72**, no. 2, R29–R36.

Fomel, S., E. Landa, and M. T. Taner, 2007, Post-stack velocity analysis by separation and imaging of seismic diffractions: Geophysics, **72**, no. 6, U89–U94.

Hardage, B. A., J. L. Simmons, D. E. Lancaster, R. Y. Elphick, R. D. Edson, D. L. Carr, and V. Pendleton, 1996, Boonsville 3-D seismic data set: Bureau of Economic Geology.

Levy, S., and D. W. Oldenburg, 1987, Automatic phase correction of common-midpoint stacked data: Geophysics, **52**, 51–59.

Longbottom, J., A. T. Walden, and R. E. White, 1988, Principles and application of maximum kurtosis phase estimation: Geophysical Prospecting, **36**, 115–138.

Saggaf, M. M., and E. A. Robinson, 2000, A unified framework for the deconvolution of traces of nonwhite reflectivity: Geophysics, **65**, 1660–1676.

Trantham, E. C., 1994, Controlled-phase acquisition and processing: 64th Annual International Meeting, SEG, Expanded Abstracts, 890–894.

van der Baan, M., 2001, Acoustic wave propagation in one-dimensional random media: The wave localization approach: Geophysical Journal International, **145**, 631–646.

———, 2008, Time-varying wavelet estimation and deconvolution by kurtosis maximization: Geophysics, **73**, no. 2, V11–V18.

van der Baan, M., and D.-T. Pham, 2008, Robust wavelet estimation and blind deconvolution of noisy surface seismics: Geophysics, **73**, no. 5, V37–V46.

Walden, A. T. and J. W. J. Hosken, 1985, An investigation of the spectral properties of primary reflection coefficients: Geophysical Prospecting, **33**, 400–435.

———, 1986, The nature of the non-Gaussianity of primary reflection coefficients and its significance for deconvolution: Geophysical Prospecting, **34**, 1038–1066.

White, R. E., 1988, Maximum kurtosis phase correction: Geophysical Journal, **95**, 371–389.

Wiggins, R. A. 1978, Minimum entropy deconvolution: Geoexploration, **16**, 21–35.

Zeng, H., and M. M. Backus, 2005, Interpretive advantages of 90°-phase wavelets: Part II — Seismic applications: Geophysics, **70**, no. 3, C17–C24.